Nigerian Research Journal of Engineering and Environmental Sciences 8(2) 2023 pp. 347-358
p ISSN: 2635-3342; e ISSN: 2635-3350

Nigerian Research Journal of Engineering and Environmental Sciences
Journal homepage: www.rjees.com

Original Research Article

Optimization of Welding and Heat Treatment Parameters for Enhanced Mechanical Performance in Micro-Alloyed Steel Components

***[1]Adzor, S.A., [1]Afabor, A.M., [2]Pullah, A. and [3]Utu, O.G.**

[1]Department of Materials and Metallurgical Engineering, Delta State University of Science and Technology, Ozoro, Delta State, Nigeria.
[2]Department of Marine Engineering, Delta State University of Science and Technology, Ozoro, Delta State, Nigeria.
[3]Department of Welding and Fabrication Engineering Technology, Delta State Polytechnic, Ogwashi-uku, Delta State, Nigeria.
*adzorsa@dsust.edu.ng

http://doi.org/10.5281/zenodo.10441775

ARTICLE INFORMATION

Article history:
Received 21 Oct. 2023
Revised 10 Nov. 2023
Accepted 10 Nov. 2023
Available online 30 Dec. 2023

Keywords:
Response surface methodology
Process parameters
Micro-alloyed steel
Impact strength
Optimization

ABSTRACT

This research study explores the significant impact of welding current and post-weld heat treatment parameters on the mechanical properties of micro-alloyed steel components in engineering structures, with a focus on ensuring their long-term durability and preventing costly failures. The investigation assesses the combined influence of welding current, tempering temperature, and soaking time on the impact strength of E7018 electrode-welded and tempered micro-alloyed steel. To optimize these parameters, response surface methodology was employed within an optimal experimental design framework, utilizing a polynomial regression model with quadratic terms and analysis of variance. The results indicate the model's strong significance (p<0.0001) in predicting the impact strength of the welded and tempered steel, with high adjusted coefficient of multiple determination (97.67%), coefficient of multiple determination (99.83%), and a predicted R-squared value (98.38%), demonstrating its precision in representing the response surface. The study identifies the optimal welding conditions for maximum impact strength as 102 A for welding current, 120 min for soaking time, and 450 °C for tempering temperature, resulting in an impact strength of 29.7 J. Through the optimization process, the highest impact strength of 29.9 J is projected under predicted conditions: 101.37 A for welding current, 120 min for soaking time, and 450 °C for tempering temperature, with minimal deviations (-0.67%) from experimental results, well within acceptable margins. This research validates the reliability of the optimization process by fine-tuning welding and heat treatment parameters.

1. INTRODUCTION

The ever-growing demand for materials with superior mechanical properties to enhance performance in challenging service environments has continues to garner research interest. Well-planned and executed experiments can lead to improved yields and performance, which are the primary objectives of any industrial setup. However, achieving this has often proven to be a significant challenge for many welding practitioners (Nweze and Achebo, 2021; Owunna and Ikpe, 2019). Various statistical tools have been developed and find widespread applications in the fields of science and engineering.

In recent years, the optimal design approach has gained significant attention in experimental design due to its ability to create tailored designs that align with specific experimental objectives, as noted in Jensen, (2018). Among the crucial factors influencing welding quality, process parameters stand out. Therefore, selecting the most suitable process parameters settings to optimize response variables within the experimental design space, while minimizing the number of experimental trials to reduce material wastage and operational costs, is of paramount importance (Nweze and Achebo, 2021). Li *et al.,* 2018 asserted in their study that predictive models offers the advantage of reducing the need for extensive physical examinations and the cost of producing new products.

Selecting the appropriate process parameters for welding operations is crucial for forming weld microstructures with excellent mechanical properties, thereby enhancing weldment performance during service. Reports by Ahmad *et al.,* (2021); Ebhota *et al.,* (2021); Sada, (2018); Kurmar *et al.,* (2018) and Tavares *et al.,* (2014) available in the public domain, reveal that welding current, welding speed, arc voltage, post weld heat treatment temperature, and soaking duration are the most influential process parameters with remarkable effects on the mechanical properties of welded metals.

Ebhota *et al.,* (2021) pointed out that many failures of welded components in service are attributed to improper selection of welding parameters. Thus, to avoid undesirable microstructures with poor mechanical properties, detrimental to the safety and integrity of welded structures in service, it is essential to screen the various candidate process parameters to determine their impact on weld properties. Zheng *et al.,* (2015) and Lawson, (2003) opined that screening of these parameters can help identify independent input parameters that maximize desired weld properties and improve productivity. Studies have shown that optimization can be achieved with the application of response surface methodology (RSM) (Suliman, 2017). RSM is a statistical and mathematical technique used to develop empirical models and optimize processes in which a response variable of interest is influenced by multiple parameters (Suliman, 2017; Myers, 2009). RSM has been extensively employed by seasoned researchers, often in conjunction with other design techniques, to enhance welding process performance, efficiently identifying process parameters with significant potential to influence the desired response variables (Lamidi *et al.,* 2023). Response surface models are constructed by fitting approximating models to the experimental data obtained in a designed experiment (Montgomery and Cook, 2009).

Ebhota *et al.,* (2021) performed optimization to enhance the toughness of mild steel welded joint and concluded that welding current had the most significant influence on the toughness. The Taguchi technique was utilized by Ahmad *et al.,* (2021) to optimize the input factors for tungsten inert gas welding of mild steel, while Fiona *et al.,* (2020) used an empirical model to optimize the welding variables for arc-welding of different metallic alloys. Sada (2018) employed the RSM to predict and optimize the welding parameters for tungsten inert welding of mild steel plate. In the optimization of welding variables for arc-welding of dissimilar metal using the tungsten gas welding process, the grey relational technique was applied by Wahule and Wasankar (2018). The results showed that the various parameters utilized had significant impact on weld properties. In Owunna and Ikpe (2019) the central composite design of experiments was applied in conjunction with an artificial neural network approach to optimize output responses for TIG-welded low-carbon steel.

A summary of the various literatures reviewed in this research work demonstrates that optimization techniques have been extensively employed in numerous research investigations to obtain suitable welding parameters for producing welds with optimal mechanical properties, thereby enhancing performance in critical service applications. However, limited literature is available in the public domain on the optimization and prediction of impact strength in micro-alloyed steel joints produced using shielded metal arc welding. Shielded metal arc welding is a conventional manual welding process widely used in industries for metal joining. Therefore, this study focuses on the optimization of process parameters and prediction of impact strength in arc-welded and tempered micro-alloyed steel. Welded components are expected to possess adequate impact strength to withstand rapid and cyclic loading, which may threaten their integrity during service.

2. MATERIALS AND METHODS

2.1. Materials and Equipment

The research study employed various materials and equipment, including the following: Micro-alloyed steel plate (5 mm thickness), Shielded metal-arc welding machine (Model: Safex M340), Electrode, Electrode drying oven, Stopwatch, Digital multimeter, Metallurgical cut-off wheel, Grinding and polishing machine, Emery papers, Etchant, Optical microscope, Scanning electron microscope, Impact testing machine and Water. The commercial grade of the micro-alloyed steel used in this research was provided by Donasula Brother's Limited, located in Warri, Delta State. The E7018 electrode was procured from the welding materials and allied products section of the Bridge Head Market in Onitsha, Anambra State. The chemical composition of both the E7018 electrode and the micro-alloyed steel was meticulously analyzed at the Engineering Materials Development Institute in Akure, Ondo State, using an EDX3600B energy dispersive x-ray fluorescence spectrometer. The results of this analysis are presented in Table 1.

Table 1: Elemental composition of test materials (wt%)

Composition	C	Si	P	S	Ti	AL	Cr	Mn	V	Nb	Zn	Cu	N	Ca	Fe
Micro-alloyed steel	0.15	0.40	0.05	0.03	0.01	0.02	0.08	0.35	0.12	0.03	0.002	0.16	1.1	0.001	97.00
E7018	0.12	0.75	0.03	0.034	0.021	0.03	0.06	0.30	0.01	-	0.001	0.13	0.04	0.002	98.00

2.2. Welding Procedure

The welding process employed the bead-on-plate technique, where weld beads were systematically deposited longitudinally along a marked straight line at the center of each plate. The plates had dimensions of 300 x 60 x 5 mm. This welding operation was carried out using the E7018 electrode with preset welding currents of 90 A, 94 A, 98 A, and 102 A.

2.3. Post-Weld Tempering Heat Treatment

Following the welding process, the metallic components underwent post-weld tempering heat treatment. This involved subjecting the materials to specific temperatures, namely 250 °C, 350 °C, and 450 °C, with corresponding soaking durations of 60 minutes, 90 minutes, and 120 minutes at each temperature. The heat treatment process was meticulously carried out in a muffle furnace, ensuring strict adherence to international standards.

2.4. Impact Test

The test samples were prepared in compliance with ASTM E23 standards as reported in Badiger *et al.,* (2017). The test was performed on a Charpy impact testing machine (Model: JB-300B/500B). Each sample featured a 1mm depth V-notch with an angle of 45 °C and a root radius of 0.25 mm. During the test, the samples were positioned on a horizontal support, with the notched face precisely opposite to the location from which a weighted pendulum was released from its resting position at a fixed height to impact each sample. The energy required to fracture each sample was meticulously recorded. This process was carried out in strict accordance with established testing standards.

2.5. SEM Analysis of Welded and Heat-Treated Samples

To investigate the structural changes in the as-welded and tempered samples, Scanning Electron Microscopy (SEM) was employed, utilizing a Phenom ProX model. The samples were carefully affixed to a sample stub coated with double adhesive and subsequently sputter-coated with a 5nm layer of gold, using the Quorum Technologies Model Q150R. Following this preparation, the samples were introduced into the SEM machine's chamber. They were examined using NaVCaM and the resulting morphology data was stored on a USB stick for further analysis and documentation.

2.6. Experimental Design and Statistical Analysis

Following a rigorous assessment of key factors, namely welding current, soaking time, and tempering temperature, an optimal experimental design was chosen because of its flexibility in accommodating various levels for each factor and for giving equal emphasis in estimating main effects and interactions. The independent parameters and their corresponding design levels, as determined by the optimal design, are detailed in Table 2. To establish the range of each independent parameter, both maximum and minimum values were selected based on preliminary studies. The welding current range (90 A, 94 A, 98 A and 120 A) adhered to manufacturer specifications. The tempering temperature range (250 ºC, 350 ºC and 450 °C) and soaking time (60 min, 90 min., and 120 min.) were chosen to strike a balance between avoiding excessive grain growth which can adversely affect impact strength. The Experiments were conducted at all designated points in a random order, with multiple replications of each factor to ensure more reliable and stable average results. The design for the Response Surface Methodology (RSM) incorporating these three factors was generated using Design-Expert version 10 software.

Table 2: Input parameters with their levels

Parameter	Unit	Range and levels			
		1	2	3	4
Welding current	A	90	94	98	102
Soaking time	min.	60	90	120	
Tempering temperature	ºC	250	350	450	

3. RESULTS AND DISCUSSION

3.1. SEM/EDS Image of Base Metal

The SEM image displayed in Figure 1 (a) reveals that the base metal comprises a combination of coarse ferrite grains. Within this ferrite matrix, there is a uniform distribution of pearlite, which is denoted by the darker patches. Additionally, there are carbide particles that are visibly segregated along the grain boundaries. These distinct phases play a substantial role in influencing the material's impact strength. The accompanying EDS spectrum image in Fig. 1(b) provides insight into the elemental composition of the material. It exhibits different elements' peaks, each of which signifies the presence of these elements at various locations within the base metal. Notably, the element with the highest peak is iron (Fe), confirming its predominance in the composition.

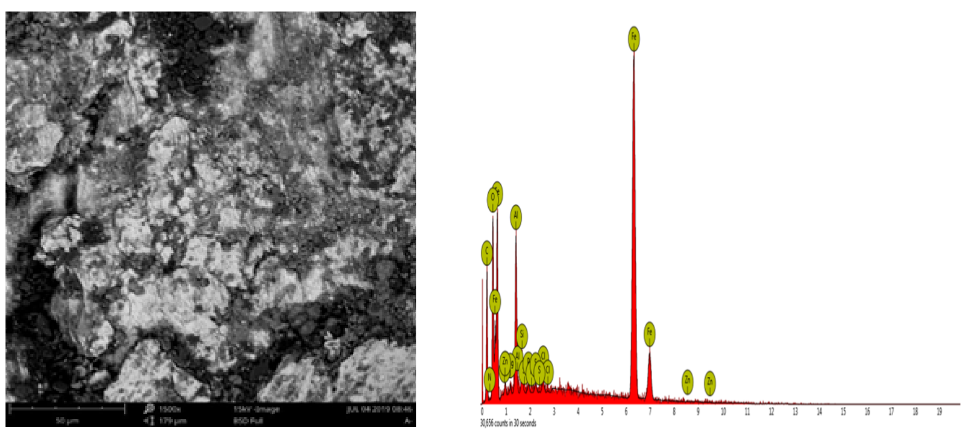

(a) (b)

Figure 1: (a) SEM image of base metal and (b) EDS of base metal

3.2. SEM/EDS Image of Weld Metal

The SEM image in Figure 2 (a) illustrates that the weld metal is characterized by a fine-grained matrix. Within this matrix, there is a consistent distribution of pearlite, which is discernible through the darker patches. Furthermore, carbide particles are finely dispersed along the grain boundaries. These distinct phases exert a significant influence on the impact strength of the weld metal. The accompanying EDS spectrum image in Fig. 2(b) offers valuable insights into the elemental composition of the material. It displays peaks for different elements, each indicating the presence of these elements at various locations within the weld metal. Notably, the element with the highest peak is iron (Fe), confirming its predominant presence in the composition.

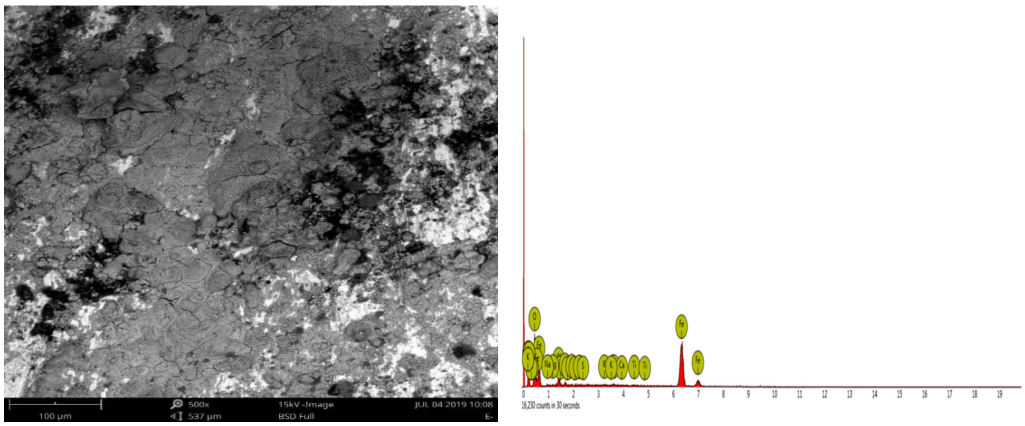

(a) (b)

Figure 2: (a) SEM image of weld metal and (b) EDS image of weld metal

3.3. Impact Strength Response Data with Corresponding Input Factors

The configuration of manual arc-welding process parameters was determined through the use of optimal design experimental methods. To ascertain the optimal settings and assess the influence of manual arc-welding and tempering process parameters on the impact strength values, an analysis of variance (ANOVA) was employed. Experiments were conducted in accordance with the parameter settings, with the response variable being the measurement of impact strength. Multiple combinations of parameters were tested, resulting in a total of 20 experimental runs aimed at maximizing impact strength. These experimental runs and their outcomes are comprehensively presented in Table 3.

3.4. Analysis of Variance (ANOVA) of Regression Model

The statistical testing of the empirical model was performed in the form of analysis of variance. The results of the analysis of variance for the fitted quadratic polynomial model of impact strength are presented in Table 4. The results indicate that the model used to fit the response variable is significant ($p< 0.0001$). The model F-value of 644.61, greater than the P-value, confirms the model significance (Shojaei *et al.,* 2021 and Shojaei *et al.,* 2021). High coefficients of regression (R^2) and adjusted regression coefficients (adj. R^2) values of 99.83% and 99.67%, respectively suggest that the model can adequately approximate the actual response data in the design space. Reports by Bradley, (2007) and Kim *et al.,* (2012) have shown that a high R^2 value does not necessarily imply a good fit because adding more parameters to the model can increase R^2 regardless of their significance. On the contrary, the adj.R^2 decreases as additional parameters are added, making it a more valid criterion for testing model fitness to the model (Hossain *et al.,* 2012). The adj.R^2 value in this study indicates that only 0.33% of the total variation could not be explained by the model. The model adequacy precision value of 84.893 implies a positive correlation between the response variable and the input parameters (Hossain *et al.,* 2012).

Table 3: Experimental design matrix for optimal arc-welded micro-alloyed steel parameters

Run	Welding current (A)	Soaking time (min)	Tempering temperature (°C)	Response (Impact strength) (J)
1	102	120	450	29.7
2	90	120	450	26.2
3	94	120	350	25.5
4	94	90	450	27.7
5	90	90	350	23.9
6	102	120	250	22.7
7	94	120	350	25.5
8	94	90	450	27.7
9	90	60	250	19.0
10	90	120	250	19.8
11	102	120	350	27.8
12	102	90	350	27.4
13	98	60	250	21.3
14	102	90	350	27.4
15	94	120	350	25.5
16	90	90	250	19.5
17	98	60	350	25.8
18	98	90	250	21.5
19	102	60	450	29.1
20	90	90	450	25.8

Table 4: Analysis of variance of regression model

Source	Sum of Square	Df	Mean square	F value	P-value Prob>F
Model	172.95	9	19.22	644.61	< 0.0001
A-Current	27.00	1	27.00	905.77	< 0.0001
B-Soaking time	1.24	1	1.42	41.56	< 0.0001
C-Temperature	120.70	1	120.70	4048.83	< 0.0001
AB	0.018	1	0.018	0.60	0.4560
AC	0.073	1	0.073	2.45	0.1483
BC	0.021	1	0.021	0.69	0.4246
A^2	0.21	1	0.21	7.08	0.0239
B^2	0.16	1	0.16	5.29	0.0443
C^2	7.07	1	7.07	237.08	<0.0001
Residual	0.30	10	0.30		
Lack of Fit	0.30	5	0.060		
Pure Error	0.000	5	0.000		
Cor Total	173.25	19			

3.5. Model Statistics Summary Output

Practical significance testing was conducted by analyzing the model summary output, as illustrated in Table 5. The coefficient of determination, along with the adjusted R-squared value, both exceeded 99%, signifying that the model parameters effectively account for the variance in the dependent variable and proficiently predict the response. Consequently, it can be inferred that the model holds considerable practical significance.

The equation for predicting impact strength in welded and tempered micro-alloyed steel, expressed in terms of coded factors representing the input parameters, is denoted as Equation (1). The coefficients within this equation serve as key indicators: the sign of each coefficient reveals the direction of the relationship, while the coefficient's magnitude signifies the strength of that relationship. The constant value for impact strength is +25.97. This value implies that when all other factors are set to zero, the impact strength is expected to be 25.97. Furthermore, the linear coefficient for welding current is +1.63, indicating that when all other factors remain constant, an increase of 1.63 in impact strength can be expected.

Table 5: Model statistics summary output

Parameter	Value
Std Dev.	0.17
Mean	25.27
C.V. %	0.68
PRESS	2.80
-2log Likelihood	-27.36
R-Squared	0.9983
Adj R-Squared	0.9967
Pred R-Squared	0.9838
Adeq Precision	84.893
BIC	2.59
AIC	17.08

Similarly, for soaking time and tempering temperature, we observe linear coefficients of +0.35 and +3.48, respectively. This implies that for every unit increase in soaking time and tempering temperature, the impact strength is predicted to increase by 0.35 and 3.48 units, respectively. The interpretation of interaction and quadratic terms follows a similar pattern, with the direction of the sign of their coefficients providing insight into their respective impacts.

$$\text{Impact strength} = 25.97 + 1.63A + 0.35B + 3.48C + 0.056AB + 0.12AC - 0.064BC - 0.26A^2 - 0.19B^2 - 1.22C^2 \quad (1)$$

3.6. Graph of Predicted Versus Actual Results

Figure 3 depicts a plot comparing the predicted impact strength values to the actual results. The graph reveals a strong positive correlation, as evidenced by the close alignment of the data points along the regression line. This close correspondence implies that the empirical model is a robust fit and possesses the capability to accurately forecast experimental outcomes, in accordance with findings from Zainal-Abideen *et al.,* (2012).

The perturbation plot is a valuable tool for assessing the impact of individual variable factors within a specific point in the design space. In this analysis, the response is charted while adjusting one factor across its entire range, while keeping all other factors constant. This technique is instrumental in identifying the factors that exert the most influence on the response (Hazard *et al.,* 2007). Figure 4 displays the perturbation plot for welding current, soaking time, and tempering temperature in relation to impact strength. The curvature observed in the profiles of these independent factors suggests their positive contributions to the response variable, which in this case is impact strength. Notably, a statistically significant probability value ($P < 0.00001$) for the input parameters (Table 4) underscores their substantial impact on the response. Furthermore, the F-values, which are 4048.83, 905.77, and 41.56 for tempering temperature, welding current, and soaking time, respectively, indicate the extent of their influence on the response. In this context, tempering temperature emerges as the most significant factor affecting the response, followed by welding current and soaking time.

Figure 5 illustrates the graphical depiction of the interaction between soaking time and temperature and their impact on impact strength. The elliptical shape of the plot signifies a clear correlation between these two variables. Notably, the graph visually conveys that optimal impact strength can be attained by elevating both interacting factors. In essence, as both tempering temperature and soaking time increase, impact strength shows a corresponding increase. This phenomenon is likely due to the increased precipitation of carbide particles and their uniform distribution in the ferritic matrix. Ahmed and Krishnan (2000) found that the temperature reached during stress relief treatment has a significantly greater effect on relieving tensile welding stresses and enhancing mechanical properties than the duration the sample is held at that temperature.

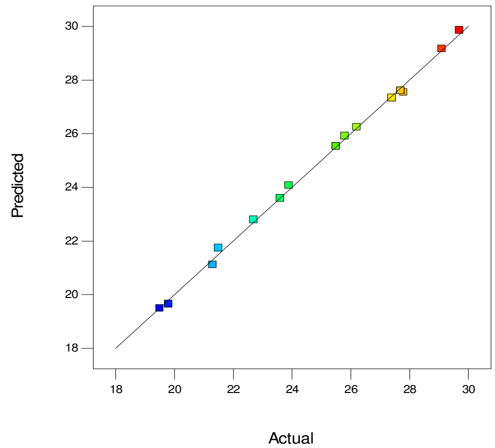

Figure 3: Plot of predicted versus actual values of impact strength

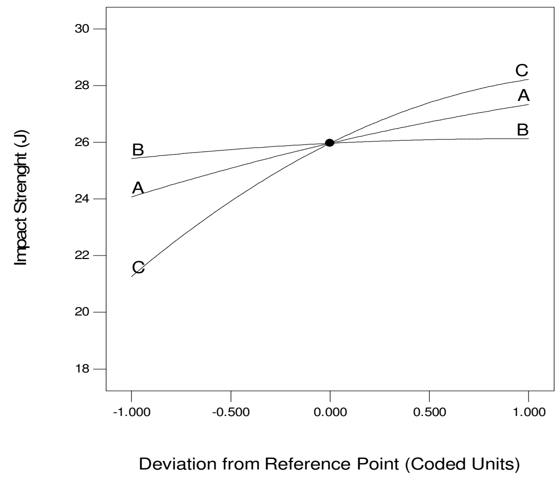

Figure 4: Perturbation plot of welding current, soaking time and temperature on impact

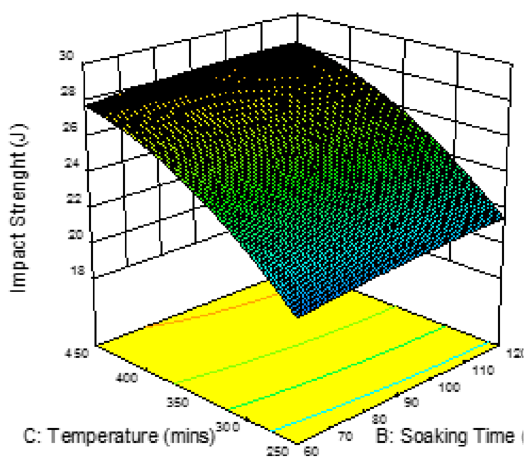

Figure 5: Response surface and contour plot of soaking time and temperature on impact strength

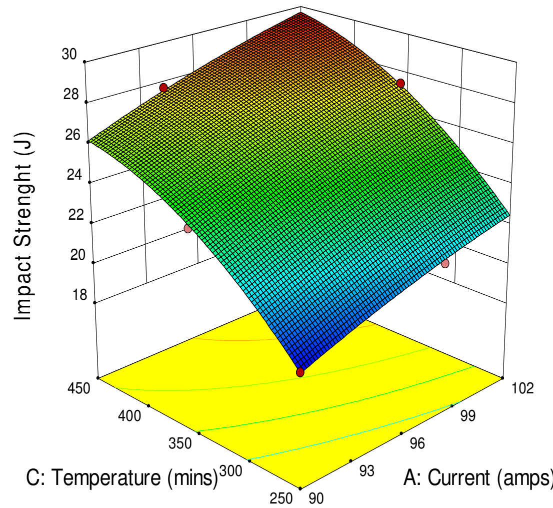

Figure 6: Response surface and contour plot showing the effect of welding current and temperature on impact strength

Figure 6 provides a visual representation of the interaction between welding current and tempering temperature and their impact on resulting impact strength. The elliptical pattern observed in the plot emphasizes the significant synergy between these process parameters and the response variable. This graph vividly demonstrates that the highest impact strength can be achieved by increasing both values of the interacting factors. Entrekin (1983) documented that as the tempering temperature increases, heat-treated steel softens, leading to increased atom spacing with a higher potential for solute atoms to be uniformly distributed to new locations within the crystal lattice. Additionally, an increase in welding current introduces more detrimental welding residual stresses into the welded components, necessitating higher tempering temperatures for effective stress relief. Internal stress relief imparts several desirable qualities to steel, including increased ductility, greater toughness, and improved impact resistance (Warner and Brandt, 2005).

Figure 7 offers a visual depiction of the interaction effect between welding current and soaking time in relation to impact strength. The plot's subtle curvature implies that the combined impact of these factors does not strongly favour a positive influence on the response variable. This inference is substantiated by the associated probability value (P > 0.1) for the interaction factors (AB) as shown in Table 4. Furthermore, the limited impact of these interacting factors on the response is attributed to the fact that extended soaking times tend to result in grain coarsening, which, in turn, can have adverse effects on the mechanical properties of heat-treated steels.

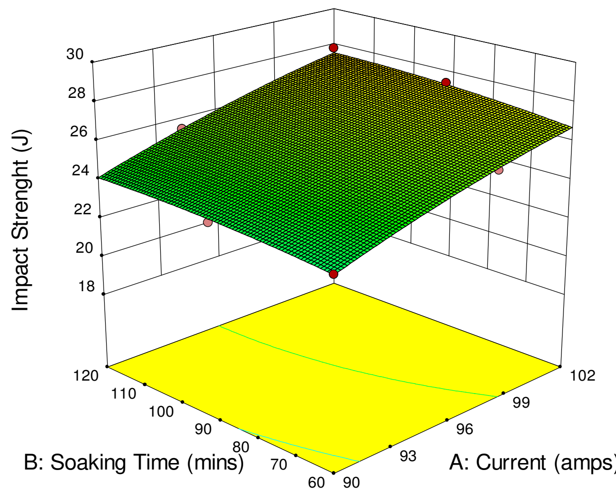

Figure 7: Response surface and contour plot showing the effect of welding current and soaking time on impact strength.

3.7. Optimization of Impact Strength

The optimization process was undertaken with the goal of determining the optimal combination of process parameters, including welding current, tempering temperature, and soaking time. This sought to enhance the response while minimizing the variability between the model-predicted and experimental results. The specific optimization criteria employed in this study are detailed in Table 6.

Table 6: Optimization criteria and bounds

Process parameter and response factor	Bounds		Criterion	Goal
	Lower	Upper		
Welding current	90	102	In range	In range
Soaking time	60	120	In range	In range
Tempering temperature	250	450	In range	In range
Impact strength	19.5	29.7	In range	Maximize

3.8. Optimal Conditions and Response Data

The optimal combination of welding current, tempering temperature, and soaking time values required to achieve the desired response is presented in Table 7. These values were determined using Design-Expert statistical software version 10 (2016). Upon examination, it was found that the selected set of combined values for the process parameters, resulting in a maximum impact strength of 29.9 J, were as follows: 101.37 for welding current, 120 for soaking time, and 450 °C for temperature. The desirability index for this optimal combination of values, as generated by the Design-Expert software, was calculated to be 0.789. In accordance with the findings of Granato and Calado (2014), a desirability index of ≥0.70 suggests that the input variables selected are appropriate and will effectively optimize the desired output.

Table 7: Optimal solution as provided by design expert software based on the criterion and goal on impact strength

Number	Current (amps)	Soaking time (min)	Temperature (°C)	Impact strength (J)	Desirability
1	101.39	120	450	28.8	0.778
2	101.37	120	450	29.9	0.778
3	101.44	120	450	28.9	0.778

3.9. Validation of Impact Strength Optimization

The experimental phase yielded a maximum impact strength of 29.7 J when the welding parameters were configured at 102 amperes, 120 minutes, and 450 °C for welding current, soaking time, and tempering temperature, respectively. In contrast, the optimization process produced the highest impact strength of 29.9 J under predicted conditions, which included 101.37 A, 450 °C, and 120 minutes for welding current, tempering temperature, and soaking time, respectively. These results showcase a remarkable alignment between the two data sets, with only slight deviations well within the acceptable range for experimental outcomes. It's noteworthy that the experimental results displayed a minor negative deviation from the predicted values (Table 8). This indicates that the actual impact strength values were slightly lower than anticipated. This deviation can be attributed to the real-world welding process, which may have influenced the material surface differently than the assumptions made during the optimization process. Additionally, it is crucial to consider the complex interactions occurring within the weld zones and their interfaces with the surrounding material during the welding process. These interactions, potentially involving physio-chemical processes, played a significant role in determining the final impact strength. Unfortunately, these intricate dynamics were not considered as criteria during the optimization process, which likely contributed to the observed deviation in the results.

Table 8: Comparative analysis of predicted and experimental impact strength at optimal conditions

Optimum condition	Welding current (A)	Soaking time (min)	Temperature (°C)	Impact strength (J)	Percentage deviation
Predicted condition	101.37	120	450	29.9	-0.67%
Experimental condition	102	120	450	29.7	

4. CONCLUSION

The research investigation yields several noteworthy conclusions:

1) The developed model for predicting impact strength in arc-welded and tempered micro-alloyed steel welds demonstrates strong statistical significance ($P < 0.0001$), emphasizing its reliability in predicting the actual response.

2) The positive contributions of the linear terms within the regression model ($P < 0.0001$) further validate the model's effectiveness.

3) Optimization efforts have established that the maximum attainable impact strength is 29.9 J, under the predicted conditions of 101.37 amperes for welding current, 450 degrees Celsius for tempering temperature, and 120 minutes for soaking time.

4) A comparison between experimental and predicted data reveals a close alignment, with deviations well within the acceptable range for experimental results.

5) This research study underscores the robustness of the optimization process, providing valuable insights for enhancing the mechanical performance of micro-alloyed steel components in engineering structures through optimized welding and heat treatment parameters.

6) Overall, the research findings endorse the efficacy of the developed model and its practical applicability in improving the mechanical properties of micro-alloyed steel welds for engineering applications. These

findings hold significance for advancing the field and contributing to the quality and performance of micro-alloyed steel components in various engineering applications worldwide.

5. ACKNOWLEDGMENTS

The authors gratefully acknowledge the invaluable support received from the Department of Industrial Metallurgy and Foundry Engineering, as well as the Welding and Fabrication Engineering Department of the Metallurgical Training Institute, Onitsha. Their expertise and skilled personnel were instrumental in successfully carrying out the crucial heat treatment and welding operations.

6. CONFLICT OF INTEREST

There is no conflict of interest associated with this work.

REFERENCES

Ahmed, J., Shaik, M., and Musthak, M. (2021). Prediction of Effects of Process Parameters to Study the Microstructure of TIG Welded Mild Steel Sheet by Taguchi Method. American Journal of Materials Science, 11(2), 37-47.

Ahmed, K., and Krishnan, J. (2002). Post weld heat treatment: Case studies. Bhabha Atomic Research Centre, Mumbai, Newsletter, 111-115.

Badiger R. I., Narendranath S., and Srinath M. S. (2017). Microstructure and Mechanical Properties of Inconel-625 Welded Joint developed through microwave hybrid heating. Proceedings of the Institute of Mechanical Engineers Part B. Journal of Engineering Manufacture, 4.

Bradley, N. (2007). The Response Surface Methodology. MSc Thesis Department of Mathematical Sciences. Indiana State University South Bend, India, 2-3, 19.

Ebhota, L. M., Ogbeide, O. O., and Abhulimen, I. U. (2021). Prediction and Selection of the Best Process Parameters to Improve Toughness of Mild Steel Welded Joints. Open Access Library Journal, 8(8), 1-9.

Entrekin, C. H. (1983). Effect of stress relief on micro-alloyed weld metal impact properties. Welding Journal, 197-203.

Fiona, C., Junting, X., Thomas, D. G., and Murphy, A. B. (2020). Model-Based Parameter Optimization for Arc Welding Process Simulation. Applied Mathematical Modelling, 81, 386-400.

Hossain, M., Majuumder, A. K., and Basak, T. (2012). An application of non-linear cobb-douglas production function to selected manufacturing industries in Bangladesh. Open Journal of Statistics, 2(4), 460-468.

Jensen, W. A. (2018). Open Problems and Issues in Optimal Design. Quality Engineering, 30(4), 583-593.

Kim, H. K., Do, J. R., Lim, T. S., Akram, K., Yoon, S. R., and Kwoon, J. H. (2012). Optimization of microwave-assisted extraction for functional properties of Vitis coignetiae extract by response surface methodology. Journal Science Food Agriculture, 543-354.

Karpagaraj A., Parthiban K, and Panmani S. (2020). Optimization Techniques used in gas tungsten arc welding process- A review. Materials Today: Proceedings, vol 27, part 3, 2187-2190.

Kumar, P., Aryo, H. K., and Verma, S. (2018). Effect of Post Weld Heat Treatment on Impact Toughness of SA516GR.70 low Carbon Steel Welded by SAW Process. International Journal for Research in Applied Science and Engineering Technology, 5(7), 971-973.

Lamidi S., Olaleye, N., Bankole Y., Obalola A., Aribike E, and Adigun I. (2023). Application of RSM in product design, development, and process optimization.

Lawson J. (2003). One-step screening and process optimization experiments. The American Statistician, vol. 57, No. 1, 15.

Li, W., Yang, W., Zhao, Y., Xu, G., and Liu, X. (2019). A New Method to Predict Mechanical Properties for Micro-alloyed Steels via Industrial Data and Mechanism Analysis. Journal of Iron and Steel Research International, 26(3), 230-241.

Montgomery, D. C., and Cook, C. M. A. (2009). Response Surface Methodology: Process and Product Optimization using Designed Experiments. John Wiley and Sons.

Myers, R. H. (2009). RSM: Process and Product Optimization using Designed Experiments (3rd ed.). John Wiley and Sons, New Jersey.

Owunna, I., and Ikpe, A. E. (2019). Modelling and Prediction of the Mechanical Properties of TIG Welded Joint for AISI 4130 Low Carbon Steel Plates using Artificial Neural Network Approach. Nigerian Journal of Technology, 38(1), 117-126.

Preskar, M., Videl, D., Vrecer, F., and Gasperlin, M. (2021). Investigation of Design Space for Freeze-Drying Injection Ibuprofen using Response Surface Methodology. Acta Pharmaceutica, 71(1), 81-98.

Sade, S. O. (2018). Optimization of Weld Strength Properties of Tungsten Inert Gas Mild Steel Welds using the Response Surface Methodology. Nigerian Journal of Technology, 37(2), 407-415.

Shojaei, S., Nouri, A., and Baharinikoo, L. (2021). Application of Chemometrics for Modelling and Optimization of Ultrasound-Assisted Dispersive Liquid-Liquid Microextraction for the Simultaneous Determination of Dyes. NJP Clean Water, 4(1), 1-8.

Shojaei, S., Nouri, A., and Baharinikoo, L. (2021). Application of Taguchi Method and Response Surface Methodology into the removal of Malachite Green and Auramine by Naxnanozeolites. Sci. Rep., 11(1), 1-13.

Suliman, R. (2017). Response Surface Methodology and its Application in Optimizing the Efficiency of Organic Solar Cell. (PhD Thesis). South Dakota State University, 4.

Tavares, S. S. M., Rodrigues, C. R., Pardal, J. M., and Barbosa, E. S. (2014). Effects of Post Heat Treatments on the Microstructure and Mechanical Properties of Dissimilar Weld of Super martensitic Stainless Steel. Materials Research, 17(5), 1336-1343.

Wahule, A., and Wasankar, K. (2018). Multi-Response Optimization of Process Parameters of TIG Welding for Dissimilar Metals SS-304 and Fe-410 using Gray Relational Analysis. International Research Journal of Engineering and Technology, 05(06), 986-993.

Warner, J. C., and Brandt, D. A. (2005). Metallurgy fundamentals. Goodheart-Willcox Company, USA, 209.

Zainal-Abideen, M., Aris M., Yusuf A., Abdul-Majid Z., Selamat A and Omar S. I. (2012). Optimizing the coagulation process in a drinking water treatment plant - Comparison between traditional and statistical experimental design jar tests. Water Science and Technology, 65(3), 501.

Zheng K., Yang R., and Hu J. (2015). A new variable screening method for design optimization of large-scale problems. International Journal of materials and manufacturing, 8(3), 693.

Design-Expert 10 Software (2016). User guide: Technical manual. Stat-Ease Inc. Minneapolis, Mn.